*Phase Transitions*, 1994, Vol. 48, pp. 15-45
Reprints available directly from the publisher
Photocopying permitted by license only



# STRAIN-RELATED MICROSTRUCTURES IN MATERIALS: A COMPUTER SIMULATION STUDY OF A SIMPLE MODEL

S. MARAIS[1], E. SALJE[2,3], V. HEINE[1], and A. BRATKOVSKY[2,3]

[1] *University of Cambridge, Department of Physics, Cavendish Laboratory, Madingley Road, Cambridge, CB3 0HE, UK*

[2] *University of Cambridge, Department of Earth Sciences, Downing Street, Cambridge, CB2 3EQ, UK*

[3] *University of Cambridge, IRC Superconductivity, Cavendish Laboratory, Madingley Road, Cambridge, CB3 OHE, UK*

A simple "atomistic" model based on the strain interaction between local state variables is found to capture the essentials of strain related structural phase transitions in non-martensitic materials. The computer-simulated thermodynamic properties of the order parameter and the related microstructures, e.g. twin boundaries, show the same characteristic features as the experimental observations which are briefly reviewed.

KEY WORDS: Strain, microstructures, computer simulation

## 1 INTRODUCTION

The purpose of the present work is a theoretical and computational explanation of the metastable textures (microstructures) often formed during structural transformations (or phase transitions). Such transformations do not occur only in martensitic metals but also in a wide variety of non-metallic materials. The case of martensitic transitions has been widely discussed. Here we refer the interested reader to Christian (1965, 1990), Bilby and Christian (1956), Tanner and Wuttig (1990), Khatchaturyan (1983), Clapp (1990), Suzuki and Wuttig (1972) and Silverstein and Clapp (1988) for the discussion of martensitic microstructures. In this paper, we shall focus largely on ferroelastics. Both groups of materials have in common that the symmetry change due to the transformation leads, in most cases, to a significant strain. This strain is called the 'spontaneous strain' when expressed as the excess quantity of the low-symmetry phase with respect to the high-symmetry phase (Aizu, 1970; Wadhahan, 1982; Salje, 1991, 1993). Materials with significant spontaneous strain are called 'co-elastic' or, if the strain orientation can be changed by external stress, 'ferroelastic' as discussed by Salje (1993).

Although both martensitic alloys and non-metallic co-elastic materials generate spontaneous strain, there are significant differences between their actual transformation behaviour. In this paper we focus on the transformation texture and we shall argue

that the strain fields in non-martensites lead to twin boundaries, tweed formation, etc., *without interface dislocations* (Barsch and Krumhansl, 1984; 1988; Krumhansl and Yamada, 1990; Gooding, 1990). Interface dislocations play a minor role in non-metallic ferroelastics because, firstly, the magnitude of the spontaneous strain ($\leq 4\%$) is small compared with most martensites (Salje, 1993) and, secondly, the structural distortions can, in general, be compensated by small atomic displacements in large unit cells. These atomic displacements are possible without breaking atomic bonds and the generation of large Burger vectors. Typical examples for the types of material we have in mind are given in Section 2.

The analysis of the transition behaviour and the texture is traditionally based on Landau-Ginzburg theory. This approach is particularly appropriate in cases in which the phase transition is generated by the softening of acoustic phonon branches (e.g. in proper, pure ferroelastics) so that the physical meaning of the order parameter of the phase transition is directly connected with the spontaneous strain (Salje, 1993). However, in most non-metallic materials, such as in many oxide ceramics (Lanten, Chain and Hener, 1986; Negita, 1989; Putnis, Salje, Redfern, Fyfe and Stroble, 1987; Salje, Palosz and Wruck, 1987; Lynden-Bell, Ferrario, McDonald and Salje, 1990, Kriven, 1990, Knorr, Loidl and Kyems, 1986), high-$T_c$ superconductors (Krekels, Van Tendeloo, Broddin, Amelinckx, Tanner, Mekbod, Vanlanthem and Deltour, 1991; Schmahl, Putnis, Salje, Freeman, Graeme-Barber, Jones, Singh, Blunt, Edwards, Loram and Mirza, 1989: Salje and Parlinski, 1991; Parlinski, Salje and Heine, 1993; Parlinski, Heine and Salje, 1993), relaxors (Cross, 1987; Salje and Bismayer, 1989), acoustooptic materials, etc., the elastic softening is not the physical origin of the phase transition. Instead one finds that ordering processes such as local cation exchanges, orientational ordering of molecules, vacancy ordering, etc., produce local atomic stresses which then lead to the collectiveness of the phase transition.

It is the purpose of this review to show how such ordering processes lead to phase transitions and to discuss how the microstructures are related to the transition process.

In order to keep the discussion as transparent as possible, we first illustrate a simple model which contains the essential features of the phase transition. Figure 1 explains with a schematic example our model of an ordering process that couples linearly to microscopic strain. We represent the local ordering process by two microscopic states ($\sigma = \pm 1$ in Fig. 1) with local stresses of opposite sign. This model is clearly the most simple one which one can easily generalize to include cases where there more than two possible ordering states, each straining the surrounding crystal structure. In $ZrO_2$, for example, the $O_2$ pairs can be oriented parallel to the $x$, $y$ or $z$ axis (Negita, 1989). The main feature is that the ordering in one cell displaces the surrounding atoms, which in turn push against their further neighbours and so on. This knock-on straining of adjacent cells leads to an ordering field for the ordering process taking place inside them. The strain thus mediates a long-ranged coupling $J_{ij}$ between the order/disorder processes taking place in the various parts of the crystal. These couplings are very complex in general, but always have the important property that they are long-ranged due to the elastic interactions. They, of course, lead to a structural phase transition below some appropriate transition temperature $T_c$ (Folk, Iro and Schwabl, 1979: Cowley, 1976).



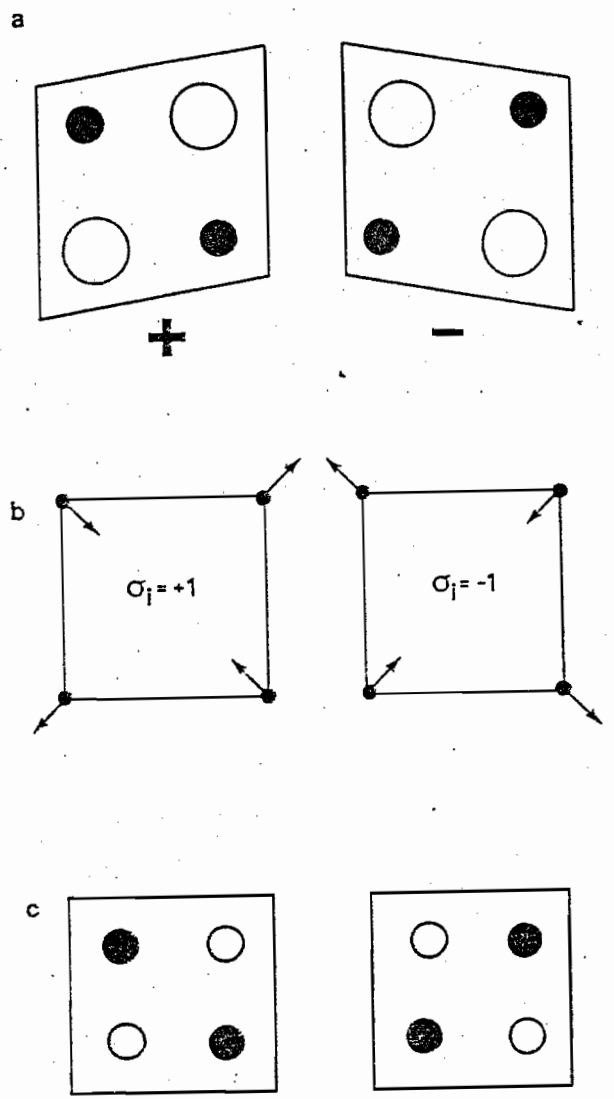


**Figure 1** Schematic drawing of the ordered structural states in (a). The two possible arrangements of the black and white "atoms" are shown as ordered (state +) and anti-ordered (state −). These structural states can be decomposed formally into a lattice distortion (b) and a configurational "iso-spin" contribution (c). The model Hamiltonian is $H = u^T A u - 2\sigma^T K u$ where $u$ is the displacement and $\sigma$ the configurational ordering variable.

The formal description of this model is given in Section 3. Using the model, we have investigated various phenomena associated with the structural phase transitions due to strain interactions, namely ferro- and antiferroelastic ordering patterns, the kinetics of ordering of such phase transitions and the metastable textures that arise during the structural phase transition. In Section 3 we shall briefly review the different types of local strain coupling and the resulting ferro- and antiferroelastic ordering patterns. Section 4 will deal with kinetics. We show that the ordering in strain-coupled systems is more or less uniform in space: each cell 'feels' every other cell due to the long-range elastic interactions. This is very different from traditional 'nucleation and growth' kinetics exhibited e.g. by models with nearest-neighbour coupling (which are much more common in theoretical studies but probably much less relevant in non-metal compounds). In some cases, however, metastable textures can form with distinct domain patterns. In order to understand these, we first discuss in Section 5 the properties of domain boundaries in strain-coupled systems. In Section 6 we give examples of the metastable textures observed in computer simulations with our model and their interpretation in the light of Section 5. This includes the formation of tweed patterns in some cases. Our conclusions are summarized in Section 7. A few preliminary results have already been discussed by Marais, Heine, Nex and Salje (1991), Parlinski *et al.* (1992) and Salje (1992a,b). A more detailed theoretical analysis of the form of the long-range coupling will be published elsewhere (Marais, Bratkovsky, Heine and Salje, 1993; Bratkovsky, Salje, Marais and Heine, 1993; Bratkovsky, Salje and Heine, 1993). Some of the essential features of tweed pattern formation have been discussed before by Bratkovsky, Salje, Marais and Heine (1993) and we refer the reader to this paper for further details.

## 2 CHARACTERISTIC EXPERIMENTAL OBSERVATIONS

We first review a few experimental observations which serve to illustrate the physical processes which are investigated in the next sections. The archetype of a ferroelastic phase transition is observed in $Pb_3(PO_4)_2$ ($R\bar{3}m - C2/c$ with $T_c = 180.1°$ C) (Salje, 1993; Bismayer and Salje, 1981: Salje, Devarajan, Bismayer and Guimaraes, 1983, Bismayer, Salje and Joffrin, 1982; Salje and Wruck, 1983, Salje, Graeme-Barber, Carpenter and Bismayer, 1993). The spontaneous strain has the components $e_{11}$ and $e_{13}$, and the linear spontaneous strain is $e_s = (e_{11}^2 + e_{13}^2)^{1/2}$. The temperature evolutiun of $e_s$ is plotted in Fig. 2a. The phase transition is almost continuous with a small first-order step at the transition point. When this crystal is held for some minutes at 2°C below the transition point, fine twinning is observed under the optical microscope which can be annealed at lower temperatures (Fig. 2b). The annealing process is essentially related to the formation of needle twins and their retraction (Fig. 2c). Such twin structures are observed in virtually all ferroelastic materials. (For coupled ferroelastic-ferroelectric domains significant modifications occur, which are not discussed here.)

As the strain formation is the most obvious feature of the phase transition, one might expect that the transition is actually driven by purely elastic instabilities.



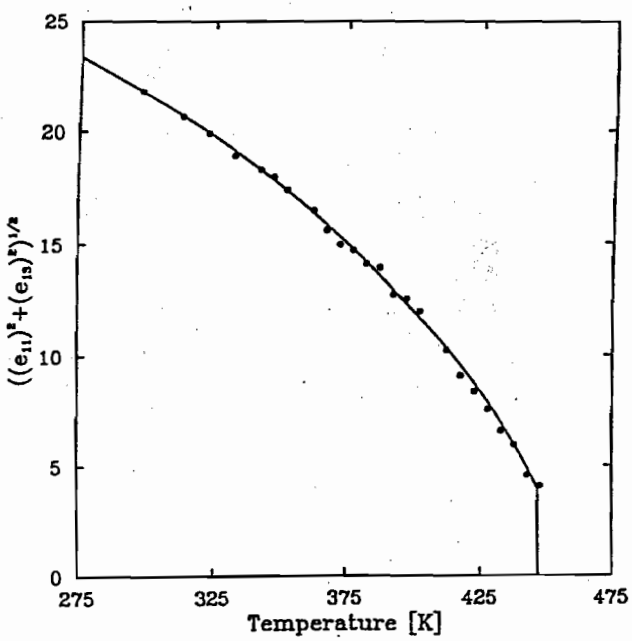


**Figure 2(a)**

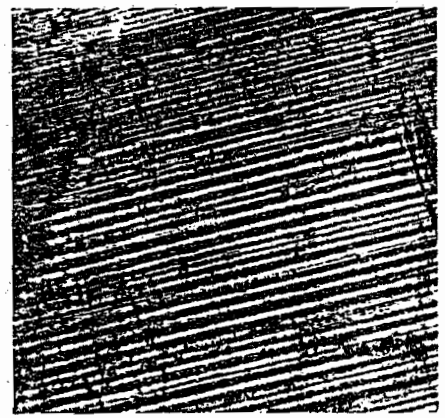

**Figure 2(b)**

Figure 2(c)

**Figure 2(a,b,c)** The temperature evolution of the spontaneous strain in lead phosphate (a). The crystal twins spontaneously (b) when cooled through the transition point. Annealing under uniaxial stress at lower temperatures (c) leads to the formation of needle twins and their retraction (length scale: 1 mm for diameter of photograph).

This, however, is not the case in $Pb_3(PO_4)_2$ nor, indeed, in most other ferroelastic materials. The transition is, in fact, generated by the off-centering of Pb from a triad axis and it is the off-centering which then couples with the strain. Roughly speaking, this means that the strain plays a dominant role for the formation of the microstructure but does not, by itself, generate the phase transition.

An example of a phase transition driven by cation ordering (i.e. an order/disorder transition) which also shows microstructures dominated by the spontaneous strain is K-feldspar (Ribbe, 1983; Kroll and Ribbe, 1987; McConnel, 1971; McLaren and Fitzgerald, 1987; Harris, Salje, Güttler and Carpenter, 1989). The structure of the ordered and disordered form of K- feldspar is shown in Fig. 3a, the typical micro structures of an ordered sample being shown in Fig. 3b. We observe again patches of highly twinned material. Apparent intersections of such twins do, in fact, not occur, but represent twins which are present in slabs superimposed along the direction of observation. The fine structure of the twins is very similar to those in Fig. 2 besides the fact that the matrix of this natural mineral is heavily warped.

In contrast to linear twin walls, antiphase boundaries of antiferroelastic materials are curved. A typical example is a mixed crystal of ilmenite-hematite (Fig. 4a) where the Fe-Ti ordering follows an anti- ferroelastic pattern (Nord and Lawson, 1989). The equivalent dark-field transmission electron micrographs are shown in Fig. 4b for various annealing temperatures. The spontaneous strain of this transition is small (0.2% at room temperature) although its influence is still visible by the oblong shape



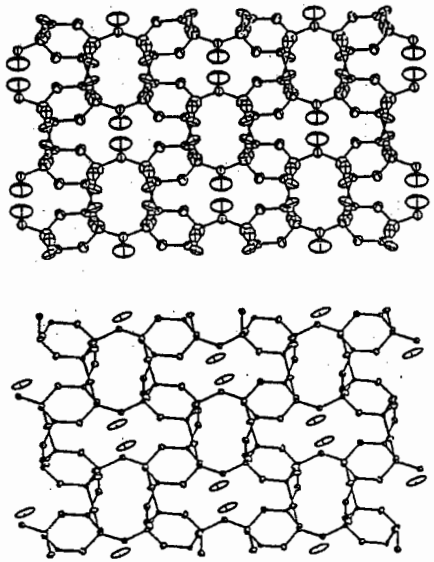

Figure 3(a)

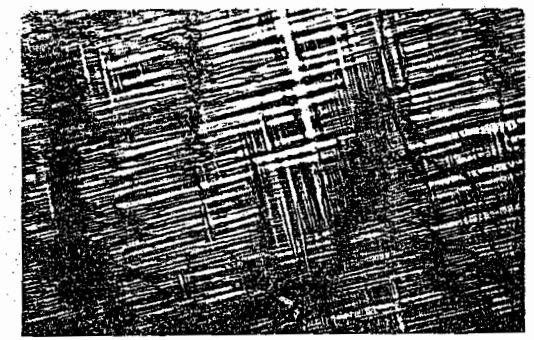

Figure 3(b)

**Figure 3(a,b)** Crystal structure disordered (top) and ordered (bottom) alkali feldspar. Note the disappearance of the vertical mirror plane during the ordering process. The typical microstructure in ordered K-feldspar (microcline) (b) shows the two dominant domain orientations perpendicular to each other. (Length scale: diameter of the figure is 1 mm, courtesy A. Putnis, Cambridge.)

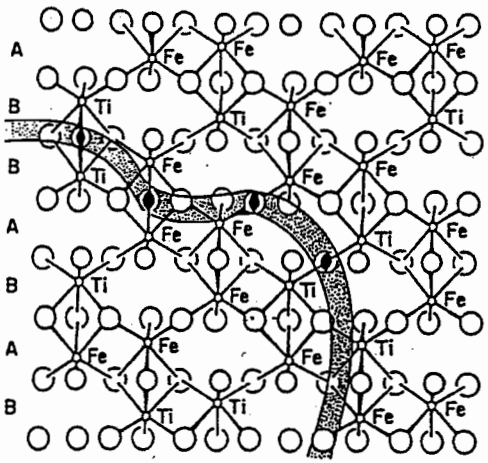


Figure 4(a)

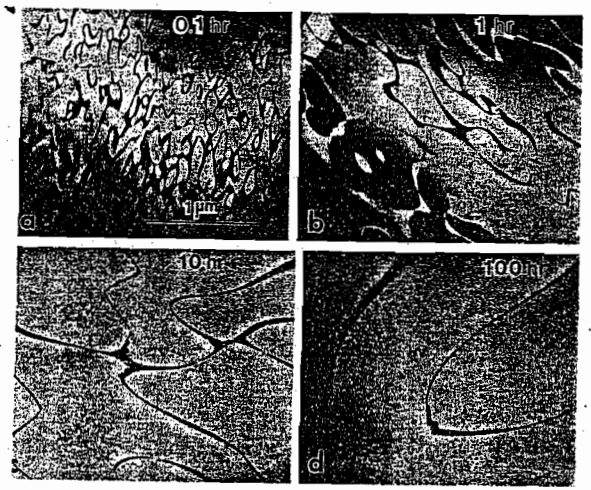


Figure 4(b)

**Figure 4(a,b)** Microstructures in ilmenite-hematite ($FeTiO_3$-$Fe_2O_3$). A domain boundary between an A-B and an B-A ordered part of the crystal is schematically shown in (a). The spontaneous strain is small. The walls are round with little preferential orientation, as found in annealed material (b) (Ilm70 annealed at 800°C, for times between 1 hour and 100 hours, courtesy of G. L. Nord, Reston).



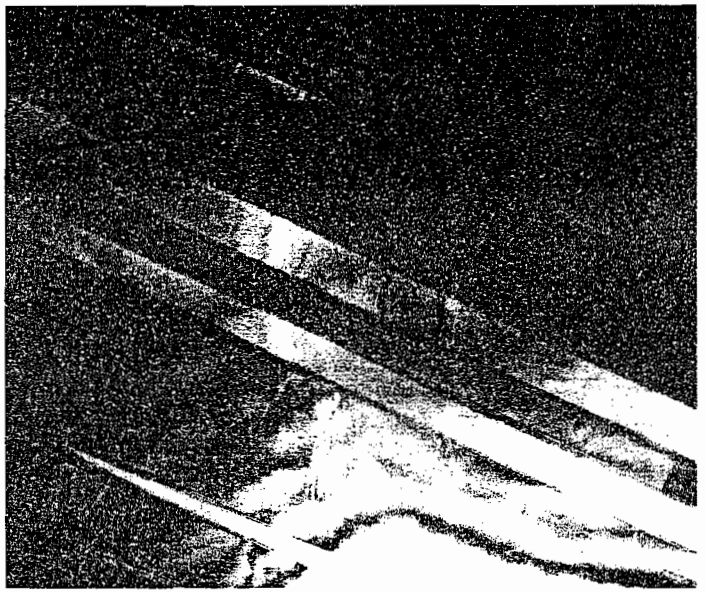

**Figure 5** Microstructure of leucite, $KAlSi_2O_6$, combining planar ferroelastic boundaries and rounded medrohedral twin walls.

of the domains. The spontaneous strain is larger in the $I\bar{1} - P\bar{1}$ phase transition in anorthite (Van Tendeloo, Ghose and Amelinckx, 1989; Redfern, Graeme-Barber and Salje, 1988) where the domains are strongly elongated along the main strain direction.

Both effects, namely linear boundaries with large strain and curved boundaries with little or no strain, can occur simultaneously in the same material. Leucite (Fig. 5) has two phase transitions at 938K and 918K ($Ia3d \rightarrow I4_1/acd \rightarrow I4_1/a$). The first transition generates ferroelastic twins whereas the second transition leads to medrohedral twinning (Palmer, Putnis and Salje, 1988; Palmer and Salje, 1990). The microstructure in the $I4_1/a$ phase contains both the linear twin boundaries and the round merohedral twins.

Finally, we give examples of the formulation of tweed patterns. In Fig. 6 the microstructure of a kinetically Al,Si disordered Na-feldspar structure (Structure as in Fig. 2a) is shown (Wruck, Salje and Graeme- Barber, 1991). This crystal was annealed at 1080°C for 8 hours. The starting materials were uniform without any visible microstructure. After annealing for longer than 20 hours under the same conditions. the microstructure disappears and the sample becomes uniform again. No significant coarsening of the microstructure was observed.

Similar tweed patterns occur also for ordering (rather than disordering) of the cations. In Fig. 7, a sequence of microstructures of increasingly Al,Si ordered cordierite

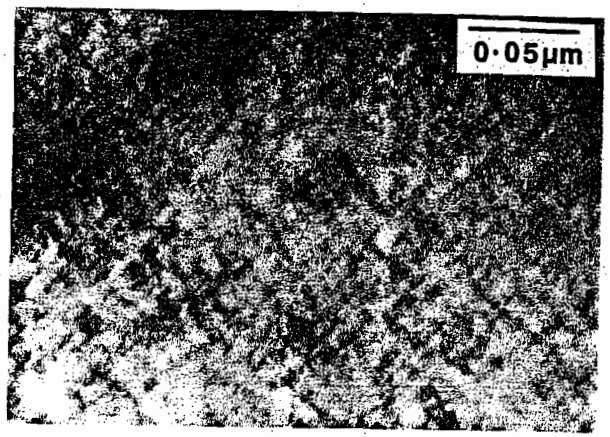


**Figure 6** Tweed-type microstructure in Na-feldspar which appears for kinetically Al. Si disordered samples. No microstructure on this length scale occurs for the fully ordered or the fully disordered material (Courtesy of A. Putnis, Cambridge).

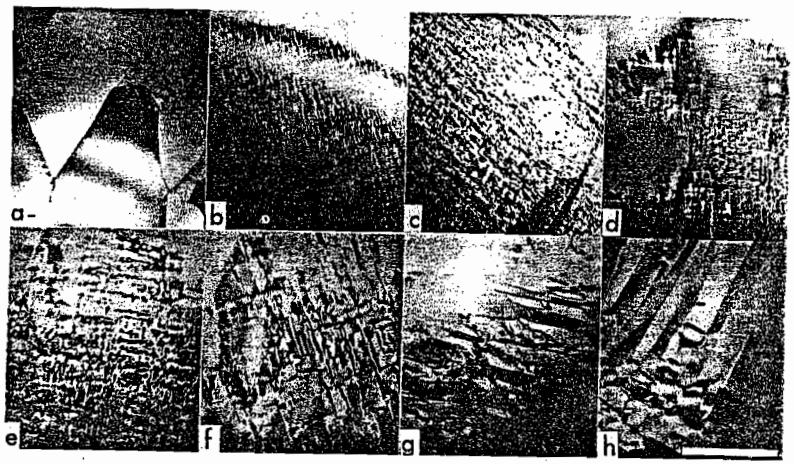


**Figure 7** Microstructures in cordierite as observed in a kinetic experiment. The homogeneous crystals in (a) are the hexagonal material without strain modulation. This phase transforms a first-order transition kinetic ally into modulated crystals (b, c, d) which show the typical tweed pattern. Orthorhombic cordierite (e, f, g, h) is highly twinned with microstructures rather similar to that of the modulated state. The macroscopic strain builds up only in the orthorhombic phase. At 1400°C the transformation is $a \rightarrow b \rightarrow c \rightarrow d$. At lower temperatures (1280°C, 1190°C) the sequence is $a \rightarrow b \rightarrow c \rightarrow e \rightarrow f \rightarrow g \rightarrow h$ avoiding the coarse nucleation in $d$ (Scale bar = 0.2μm, courtesy of A. Putnis, Cambridge).



is shown (Putnis *et al.*, 1987; Salje, 1987). The material with no long-range order (and hence no strain) is uniform. With increasing order, first tweed structures appear which then transform into twinned material.

So far we have illustrated some of the relevant features of strain-related phase transitions in which ordering processes are relevant. We now quantify the model and relate the observation to our theoretical findings, which can explain the occurrence of these different textures.

## 3 OUR MODEL AND ITS PHASE TRANSITIONS

A simple microscopic model describing the effects of linear strain interactions in structural phase transitions is now introduced. It consists of a simple cubic structure of atoms coupled via harmonic springs to one another. This structure represents in simplified form all the atoms of the system. Inside each unit cell we imagine an ordering process such as that in Fig. 1. It is not specified in further detail, but is assumed to have only two states specified by ordering various $\sigma_i$ in cell $i$ taking on the values $\pm 1$. This ordering variable couples bilinearly to the eight atoms surrounding it, i.e. there is some deformation pattern on the structure as shown in Fig. 1.

Schematically, the energy of our system can be written as

$$H = u^T A u - 2\sigma^T K u \tag{1}$$

where $u$ denotes a column vector containing the atomic displacements $u_i$, A is the dynamical matrix of coupling among the atoms and $\sigma$ a column vector of the ordering variables. $K$ couples the ordering to the atomic displacements, i.e. it represents the forces on the atoms as in Fig. 1 b. By making the transformation

$$\bar{u} = u - A^{-1} K^T \sigma \tag{2}$$

equation 1 becomes

$$H = \bar{u}^T A \bar{u} - \sigma^T J \sigma \tag{3}$$

with

$$J = K A^{-1} K^T \tag{4}$$

The interpretation of these equations is as follows. For any given state of order or disorder designated by the $\sigma_i$, the atoms at zero temperature will be in equilibrium at positions displaced from the perfect lattice sites by an amount equal to the second term in Eq. 2. Thus $\bar{u}$ is the displacement field from such equilibrium positions. The transformed Hamiltonian in eq. 3 is then the sum of two separate parts, one written in terms of a set of displaced oscillators denoted by $\bar{u}$ and coupled by the harmonic dynamical matrix, and the other as the ordering variables coupled to one another by the strain-mediated interaction matrix $J_{ij}$. Note that there is no coupling between the

two parts of the Hamiltonian or the two sets of variables. We can therefore ignore the lattice dynamics involving the $u$'s and focus purely on the ordering variables $\sigma$. The main point is that in eq. 3 the strain has introduced an effective coupling $J_{ij}$ between the $\sigma$'s. Equation 4 should be treated as symbolic and the precise nature of the $J_{ij}$ depends sensitively on the boundary conditions imposed on our model system (Gridnev, Shevelov and Bondarenko, 1985). We shall be interested only in systems with free boundaries.

The behaviour of $J_{ij}$ with free boundary conditions is discussed in detail by Marais *et al.* (1993) and we shall just recapitulate the major results. The possible $J_{ij}$'s resulting from the coupling between the ordering and the atomic displacements in our model can be divided into two classes. The six local deformations with the same symmetry as the six macroscopic strains $e_{xx}$ etc., or any linear combinations of them, form Class 1. They give a positive total coupling

$$J_{TOT} = \sum_{i \neq j} J_{ij} \tag{5}$$

where we have a single sum over all lattice positions except $j$. Class 1 couplings result in ferroelastic phase transitions. All other couplings fall into Class 2. The latter give $J_{TOT} < 0$ and structural phase transitions with the order parameter having a wavevector at the Brillouin zone boundary (Powell and Gerlach, 1989; Fleury, Scott and Worlock, 1968; Salje, 1992b, 1990, 1993) Both types of strain coupling make $J_{ij}$ long-ranged. In both cases, the $J_{ij}$ have a short-ranged part that tends to vary somewhat erratically and even oscillates in sign. At intermediate distances they fall off as $r_{ij}^{-3}$ and $r_{ij}^{-5}$ respectively, multiplied by the appropriate angular dependent parts. In Class 1 strain couplings, there is also a constant term independent of distance (i.e. of infinite range), in magnitude inversely proportional to the size of our system so that its total contribution $J_{TOT}$ is finite.

The model developed so far is clearly an oversimplification of the true experimental situation, although we believe it captures the essential physical features correctly. Modifications are necessary when several strain components interact, or when the strain field is itself not a linear response to the ordering mechanism (Salje, 1993; Plavida and Salejeva, 1988; Dove and Powell, 1989).

We also have to exclude certain situations of the following type (Folk *et al.*, 1979; Cowley, 1976; Mayer and Cowley, 1988). Consider a material with tetragonal or higher symmetry, and an ordering process which can have, say, the symmetry of an $x$ or $y$ displacement. If there is a high degree of anisotropy, the system will order locally approximately in the $\pm x$ or $\pm y$ senses which can be treated as four discrete components. However, with weak anisotropy the ordering can be any linear combination of the $x$ and $y$ types in a way that swings around slowly and continuously in direction. The latter situation would be described by a two-dimensional order parameter and cannot be treated by our simple model, although the relevant generalization appears to be straightforward.

Our strain-coupled model, without any other couplings (e.g. no direct nearest-neighbour couplings between the ordering variables), gives phase transitions as



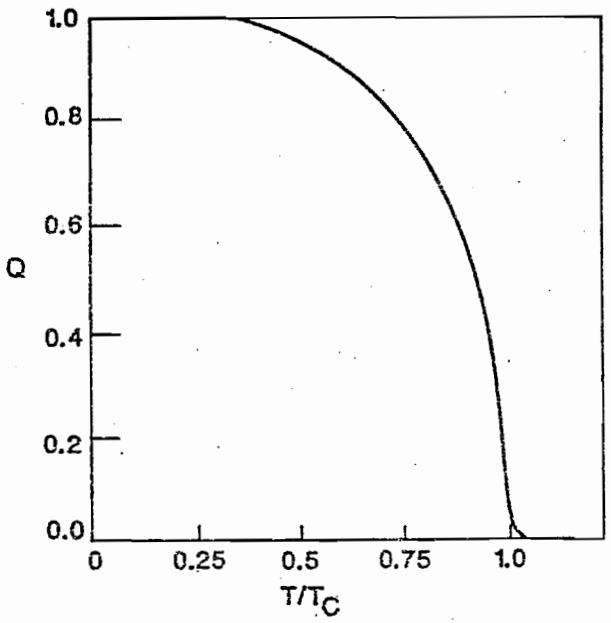


**Figure 8** Temperature evolution of the order parameter in a computer simulated model with volume strain coupling (thick line) and in mean field theory (thin line).

expected, as has been verified by computer simulations. We simulated the model as a three-dimensional $16 \times 16 \times 16$ lattice. We used a mixture of Monte Carlo techniques to find the behaviour of the ordering variables and Molecular Dynamic Simulations to calculate the new equilibrium positions of the atoms after each Monte Carlo step has changed the values (and accompanying atom forces) of some ordering variables. The temperature dependence of the order parameter, defined as

$$Q = \frac{1}{N} \sum_i \sigma_i \tag{6}$$

for ferroelastic phase transitions, also follows the behaviour of mean-field theory very well, as seen in Fig. 8. This is to be expected in the light of the $J_{ij}$'s long range. Finally, also note that our present model can be used to model impurity and exsolution problems if we add the extra constraint that the number of local ordering variables with positive sign stay constant (Cook and de Fontain, 1969, Khatchaturyan, 1966; Wagner, 1988; Mayer-Botzel and Wagner, 1988).

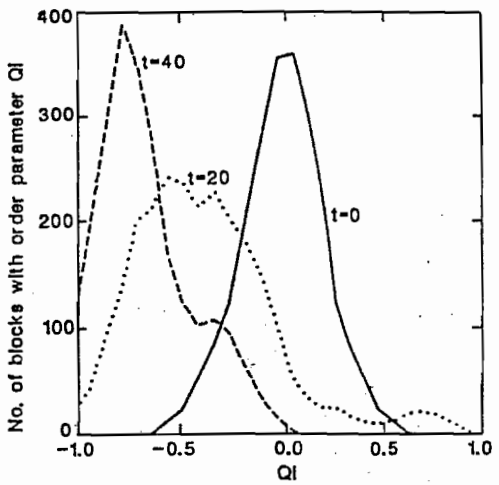


**Figure 9(a)**

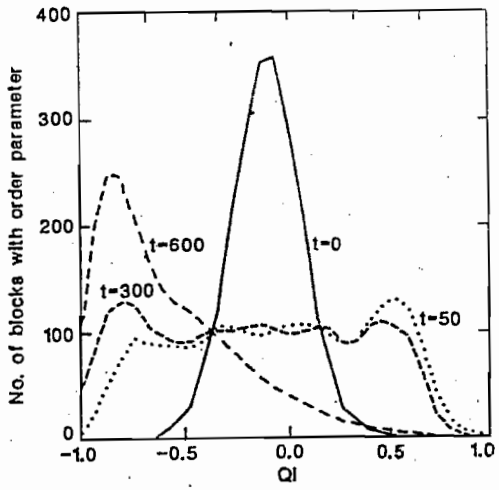


**Figure 9(b)**

**Figure 9(a,b)** Profiles of the number of 3 × 3 × 3 subblocks with a certain value of $Q_i$ in our computer model after quenching from far above $T_c$ to around $0.9T_c$. Different profiles correspond to different times after the quench in units of Monte Carlo step per ordering variable. (a) Direct nearest neighbour coupling between the ordering variables $\sigma_j$ (b) Strain coupling of the type $e_{xy}+e_{yz}+e_{yy}$ only.



## 4 KINETICS OF ORDERING

The kinetics or ordering in our strain interaction model differs from that predicted by 'nucleation and growth' theories and observed in nearest neighbour Ising models (e.g. Gunton, Gawlinski, Chakrabati and Kaski, 1988; Ogzall and Lorenz, 1988). The long-range elastic interactions couple all the local ordering variables to one another, resulting in a 'uniform' ordering of the system. We shall demonstrate this fact by computer simulations. In Fig. 9 the distribution of a coarse-grained order parameter $Q$ is shown as the system orders. The coarse-grained $Q_i$ is the average of $\sigma_i$ over the block of 3 × 3 × 3 cells centred on cell $i$. Initially $Q_i$ is distributed around zero with a statistical width of $1/\sqrt{27}$ as expected from the 3 × 3 × 3 coarse graining. Fig. 9a shows the behaviour of conventional Ising system with nearest-neighbour coupling. At $t = 50$ the system has evolved a broad distribution showing substantial clusters forming with $Q_i$ near to the equilibrium values

$$Q_i = \pm Q_{eq} \approx \pm 0.8 \tag{7}$$

with the boundaries between these regions accounting for the distribution in between the two values $\pm Q_{eq}$. Only after a very much longer time do the clusters with negative $Q_i$ (in this particular simulation) grow at the expense of the positive ones to give the final ordered state, not yet fully reached at $t = 600$.

This contrasts sharply with the behaviour of the strain-coupled system shown in Fig. 9b. Throughout the ordering process the system remains essentially uniform with the distribution retaining the form of a narrow peak. As the ordering evolves, this peak moves relatively uniformly to its value at $Q_{eq}$ (negative in this case). There are no signs of the 'nucleation and growth' processes observed in Fig. 9a.

Having shown that the sample orders uniformly, one can develop a theory of ordering kinetics (and disordering kinetics on shock heating) which leads to relatively simple rate laws describing the order parameter growth. The theory is discussed in detail by, e.g., Ginzburg and Landau (1950), Salje (1988), Dattagupta, Heine, Marais and Salje (1991), Marais and Salje (1991) and Salje and Marais (1992) and experimental results in various mineral systems confirm the theoretical approach.

Although the uniform ordering as just described is observed in our computer simulation for some systems, in other cases (i.e. for other patterns of forces $K$), we may observe a metastable or transient microstructure depending on the system and the rate of cooling. The formation of these microstructures is discussed in detail in Section 6. However, these microstructures are generally quite coarse and one may think of the ordering process as being uniform inside each separate domain.

## 5 THEORY OF DOMAIN BOUNDARIES IN OUR MODEL

In most systems metastable domains of different ordering (and strain) are formed if the system is cooled through the critical temperature. We now discuss the nature of the

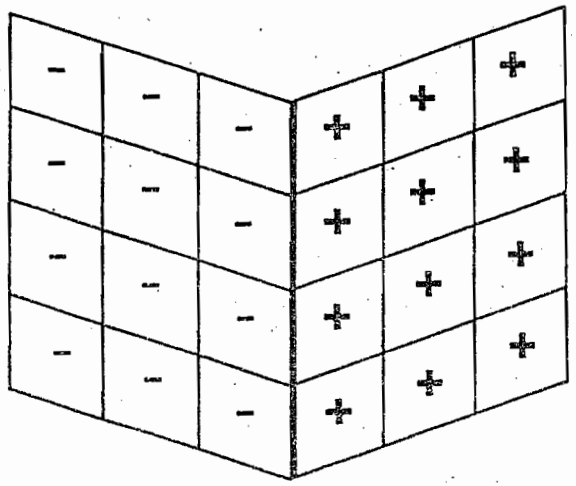

Figure 10(a)

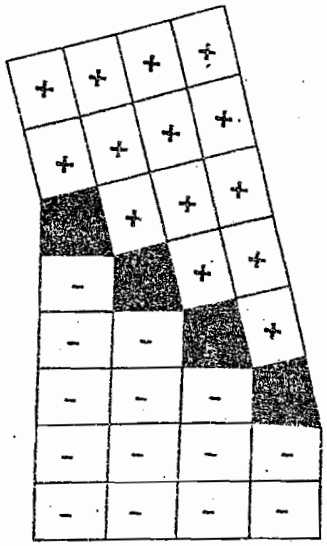

Figure 10(b)

**Figure 10** (a) Domain wall of zero-energy (type 1) for $e_{xy}$ strain coupling. Local distortions are needed to form a domain wall for $e_{xx}-e_{yy}$ coupling (b).



domain walls separating the domains in our model. Consider first the Class 1 systems (order parameter coupling to a macroscopic strain). A general criterion when crystal geometry allows two domains with different macroscopic strains $e_{ij}^{(1)}$ and $e_{ij}^{(2)}$ to have a coherent domain wall between them was described by Sapriel (1975):

$$(e_{ij}^{(1)} - e_{ij}^{(2)})x_i x_j = 0\,, \tag{8}$$

where $x$ gives the coordinates of a point in the domain wall. Eq. 8 describes a conic surface in general and a flat domain wall is possible only if the conic surface described by eq. 8 degenerates into a pair of planes. This is true if and only if $e_{ij}^{(1)} - e_{ij}^{(2)}$ is both traceless and has

$$\det|e_{ij}^{(1)} - e_{ij}^{(2)}| = 0\,. \tag{9}$$

The resulting two planes in that case give the possible orientations of the domain walls and they are always perpendicular to each other with respect to the coordinate system of the high-symmetry phase. The spontaneous shear strain in the low-symmetry phase leads to angles between walls of $\pi - 2\omega$ where $\omega$ is a measure of the spontaneous strain (Salje, 1993).

A Class 1 coupling of symmetry $e_{xx} - e_{yy}$ satisfies the criterion and hence results in compatible domain walls, as does a system with $e_{xy}$ coupling. However, not all Class 1 couplings satisfy the compatibility criterion and the tetragonal shear $2e_{zz} - e_{xx} - e_{yy}$ is such an example.

The domain walls in our model can be further subdivided into two types. A type 1 wall has zero domain wall energy, because each cell has the correct macroscopic strain right up to the boundary, as shown in Fig. 10a for the (1, 0, 0) wall for a coupling of $e_{xy}$ symmetry. As there is no domain wall energy, the driving force for domain coarsening disappears and we observe a very fine domain pattern. The fact that the type 1 walls have identically zero energy is an oversimplification due to our model, and a more complicated crystal structure or any direct interaction between the ordering variables or atom-atom interactions of longer range than next nearest-neighbour will lift this degeneracy. Nevertheless, materials with $e_{xy}$ strain (e.g. betaine arsenate discussed by Maede, 1988 and Weber, Topfield and Liabo, 1975) may tend to form relatively fine domain structures. Other walls do have a finite wall energy because there is necessarily a layer of distorted cells along the boundary as shown in Fig. 10b for the (1, 1, 0) boundary in our model with $e_{xx} - e_{yy}$ coupling. They will be called type 2 walls.

The antiferroelastic Class 2 systems can always form domain walls. In this case the local distortions do not result in a macroscopic strain and domain walls are always allowed. Furthermore, the walls can be in any direction and can be curved as well. A typical example in a Class 2 system of a domain wall generated in a two-dimensional version of our model is shown in Fig. 11. Class 2 domain walls always cost some energy, since local distortions of the unit cells are unavoidable.

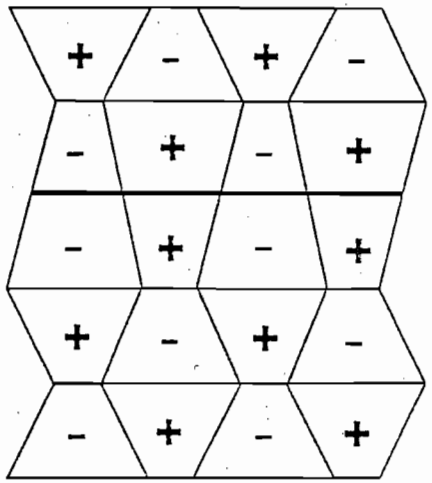


Figure 11(a)

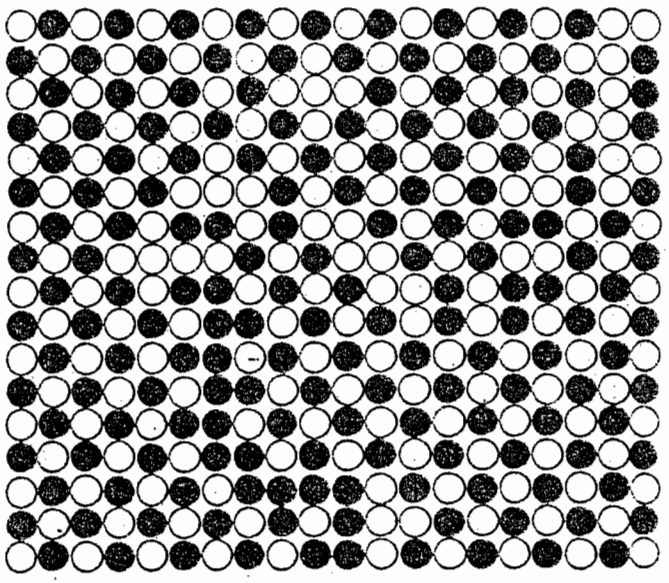

Figure 11(b)



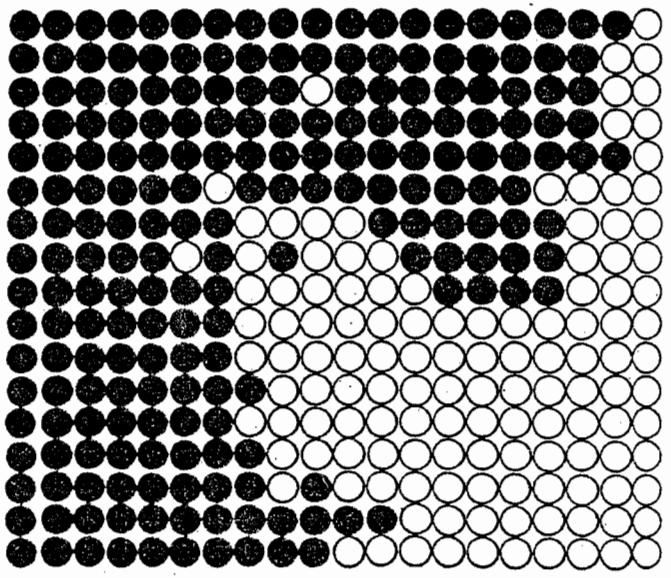

Figure 11(c)

**Figure 11(a,b,c)** Computer simulation of an antiferroelastic domain wall with strain deformations as shown schematically in (a). The thick line represents a wall. The ordering values $\sigma=+1$ are represented in (b) as black circles and $\sigma=-1$ as white circles. Walls occur where the alternation black-white is interrupted. The actual walls can be made more visible if the ordering variables are multiplied by a phase factor $\exp[i\pi(x+y)]$ so that ordering appears as black and anti-ordering as white circles (c) The same domain boundaries appear now between black and white regions.

Domain walls with structure like that in Fig. 10b are very common in minerals. A brief discussion of their properties is thus in order. In Fig. 12 we show the typical time evolution of such a wall in our computer simulation with $e_{xx} - e_{yy}$ strain coupling. Initially all ordering-variables above a (1, 1, 0) plane through the middle of the sample were set positive and all those below negative. The atomic arrangement was then allowed to relax, the ordering variables changed using the Monte Carlo techniques mentioned earlier, and the whole process iterated. We measured the average value of the ordering variable over planes perpendicular to the (1, 1, 0) direction with $Q(r)$ the average over a plane a distance $r$ from the central plane originally dividing our system in two. Because of the smallness of our sample we could only study walls at temperatures below about $0.75T_c$. Above that temperature, the wall was usually destroyed by fluctuations. As can be seen in the figure, the walls are quite narrow far below $T_c$. More than 5–6 unit cells from the centre of the wall there is very little spatial variation of $Q(r)$. The walls are also virtually motionless. Even after

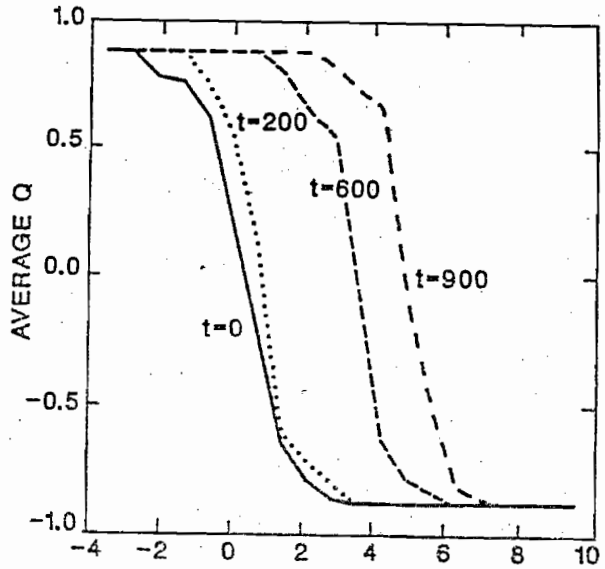


Figure 12(a)

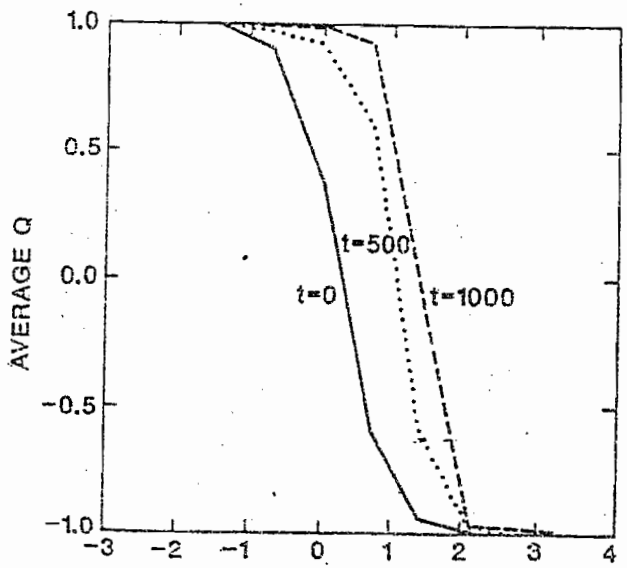


Figure 12(b)



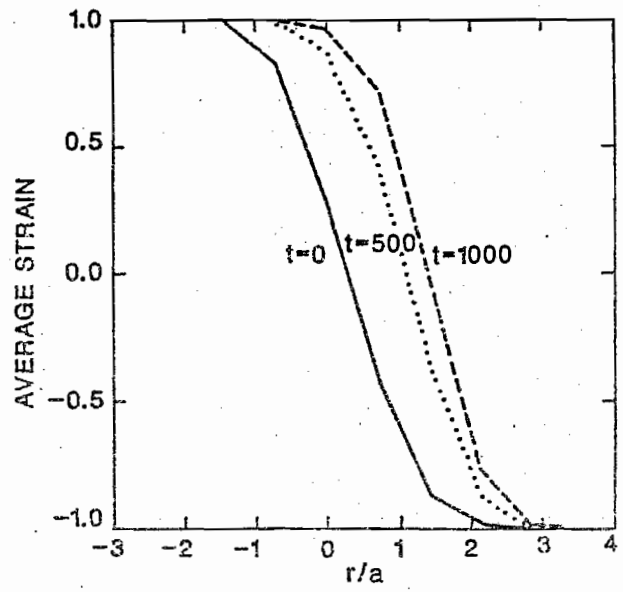


Figure 12(c)

Figure 12(a,b,c) Time evolution of a single soliton wall in the (1, 1, 0) direction in a three dimensional computer model with $e_{xx}-e_{yy}$ coupling. The values Q(r) are the average values of the ordering variables over the (1, 1, 0) planes a distance $r$ from the central plane dividing our model in half. One unit of time corresponds to one Monte Carlo step per unit cell. (a) $T = 0.7T_c$, (b) $T = 0.3T_c$. In (c) the values of the unit cell strains are shown for $T = 0.3T_c$. The strain-related profile (c) is slightly wider than for the state variable in (b).

1000 Monte Carlo steps per ordering variable, the wall has moved only a few unit cell lengths. Close to $T_c$ things may be different, but a larger simulation (currently under way) will be needed to yield this information.

## 6 METASTABLE TEXTURES

In order to investigate the formation of different domain textures, we ran a whole series of different computer simulations of our model system, whose results can be understood in terms of Section 5. In cases where the strain coupling does not obey compatibility criteria, only single domains were observed, as expected. In systems forming type 2 walls (with ferroelastic $e_{xx} - e_{yy}$ coupling for example) one of two things was observed as the system was cooled. Usually only a single domain formed in our small $16 \times 16 \times 16$ sample. However, sometimes a domain wall formed in the system of the type discussed in Section 5: it was then very stable. With $e_{xy}$ strain coupling, on the other hand, a very finely striped domain structure 1–2 unit cells wide formed, as in Fig. 13a, perpendicular to either the $x$– or $y$-axis. The fineness of the structure is due

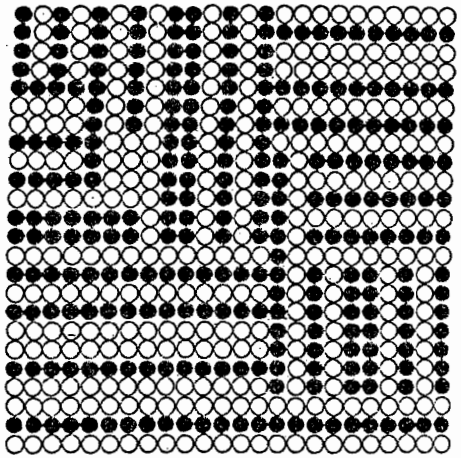

Figure 13(a)

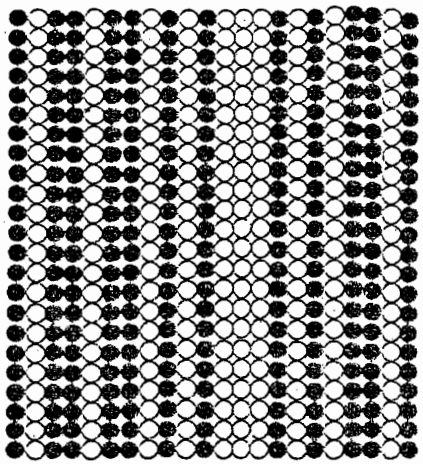

Figure 13(b)

**Figure 13(a,b)** The typical domain structure found for our model with $e_{xy}$ coupling if (a) cooled slowly and (b) quenched rapidly.



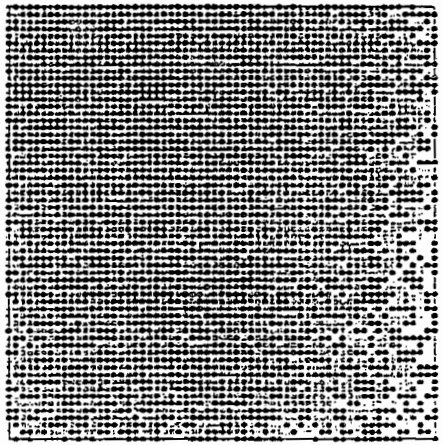

Figure 14(a)

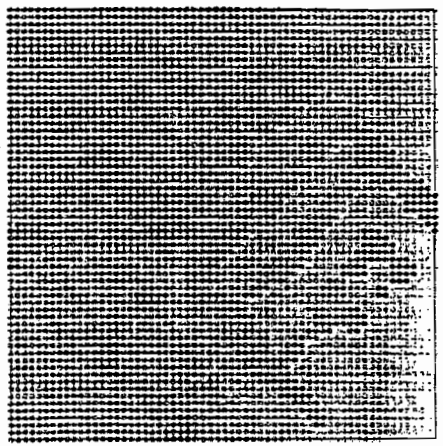

Figure 14(b)

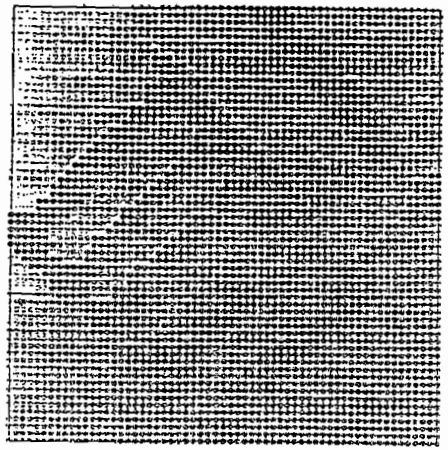

Figure 14(c)

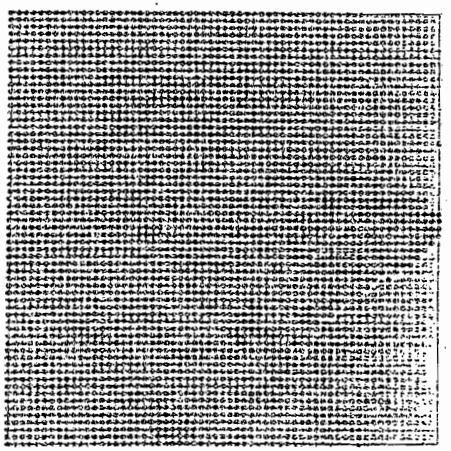

Figure 14(d)



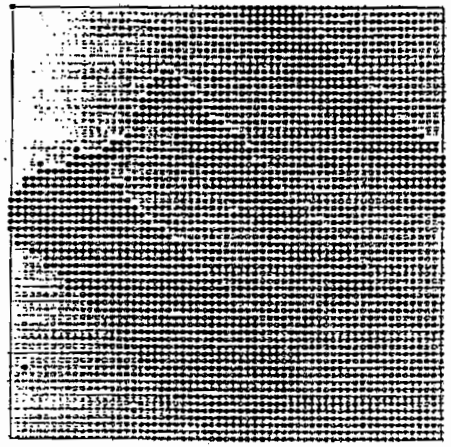

Figure 14(e)

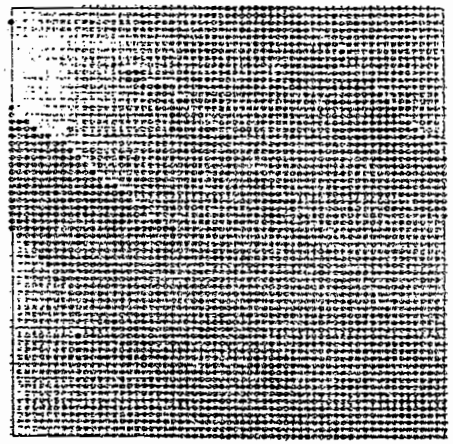

Figure 14(f)

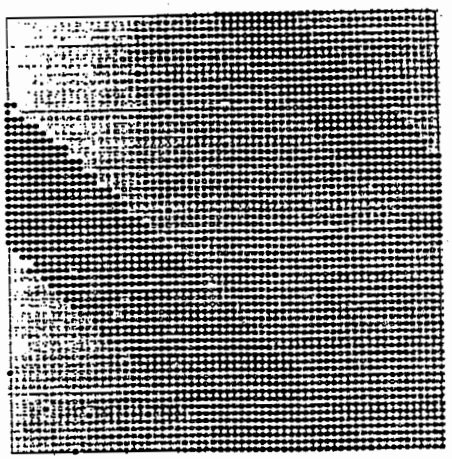

**Figure 14(g)**

**Figure 14(a,b,c,d,e,f,g)** A series of ordering variable distributions for quenches of 64 × 64 two dimensional system with $e_{xx}-e_{yy}$ strain coupling. A black circle indicates a positive value of the ordering variable, while a grey circle indicates a negative value of $\sigma_i$. If the high temperature random state (a) is quenched to below $T \approx 0.5T_c$, we observe (b) a fine tweed structure developing with walls preferentially in the [1, 1] or [1, $\bar{1}$] directions. The tweed then coarsens as time progresses and the [1, $\bar{1}$] walls start to dominate (c)–(e), until only walls in the [1, $\bar{1}$] direction are left (f). The thin wall not spanning the whole system disappears, leaving (g) a stable striped system.

to zero energy cost of a domain wall in our model. If quenched rapidly a fine tweed structure developed, with walls in both directions starting to form and the system 'getting caught' in a local minimum of the energy, looking as in Fig. 13b. When a weak direct nearest-neighbour interaction between the ordering variables $\sigma_i$ was added in the simulation, the stripes were found to broaden with increasing direct coupling. The same effect is expected with long-ranged direct atom-atom couplings (i.e. with longer than next-nearest-neighbour springs connected atoms). In fact, in this case the type 1 walls resemble type 2 walls apart from the fact that the observed microstructures are finer.

Our three-dimensional computer model is too small to study the formation of microstructures in systems with finite wall energy, since it barely allows one domain wall. We thus simulated a two-dimensional version of our model on a 64 × 64 array with $e_{xx} - e_{yy}$ strain coupling. This model may be directly relevant for the description of the CuO planes in high-$T_c$ superconductors. We believe it also describes a three-dimensional material with tetragonal symmetry where the ordering is uniform in the $z$ direction. Upon cooling from above to below $T_c$ the following behaviour (shown in Fig. 14) was observed. First, the disordered system quickly orders on a local scale



upon cooling. However, different domains with different strains form, separated by domain walls in either the [1, 1] or [1, –1] directions. After a short while a type of tweed pattern develops. Similar tweed patterns have been observed by Finlayson (1988), Wen, Khatchaturyan and Morris (1981) and Tautz, Heine, Dove and Chen (1991) using computer simulations of rectangular blocks in an isotropic medium, but we believe that our simulation gives a more detailed and more realistic atomic picture. Note that although the criteria for domain walls allow both [1, 1] and [1, –1] walls, crossing of two walls costs an extra amount of energy. For this reason one type of domain wall (in this case the [1, –1] wall) starts to dominate, until we are left with a striped system with walls in only one direction. The needle domain not spanning the whole system is now also destroyed, because of the high energy cost at its tips. Once the system has reached the final striped state, it is extremely stable, as already discussed in section 5.

Antiferroelastic walls form in any direction and are typically curved as in Fig. 11. They are also much more mobile than Class 1 walls since much less energy is needed to deform a wall locally. Temporary deformations are necessary if a wall wants to move. In a relatively short time a Class 2 wall can thus move a large distance as well as change its shape. This has also been observed in our simulations. Secondary strain coupling can result in Class 2 walls becoming flatter, such as is shown in the case of $Pb_3(PO_4)_2$.

## 7 CONCLUSION

We have presented a simple model which captures almost all of the essential characteristics of systems with strain coupling undergoing phase transitions. The essential physics in a wide variety of materials is that the strain coupling always mediates a long-range interaction between the local ordering processes. This long-range interaction leads to a uniform ordering of the system if it is disturbed from equilibrium, which makes the use of kinetic rate laws to describe the kinetics of strain-coupled systems feasible (Salje and Marais, 1992).

The main point of the work is that the kinetics can also lead to various types of textures like tweeds and stripes as shown by computer simulation. They are remarkably similar to textures observed experimentally. These textures are directly related to the elastic long-range coupling, and we have shown how their form, direction, scale, and when they do and do not occur, can be understood in terms of the structure of the domain walls.

Finally we want to return to the point that our grossly simplified model does contain the essential physics of a wide range of structural phase transitions some of which may at first sight look very different. Fig. 15, for example, shows a two dimensional representation of the perovskite structure. It can undergo a tetragonal phase transition through a coherent rotation of the octahedra (Fig. 15b), the local ordering variable being the angle of rotation $\theta_i$ which corresponds to the $\sigma_i$ of the model. Now consider what would happen when one rotates a single octahedron only. Since the octahedra are joined by shared oxygen atoms, the adjacent octahedra would be severely distorted. setting up strong internal forces within them. These forces are

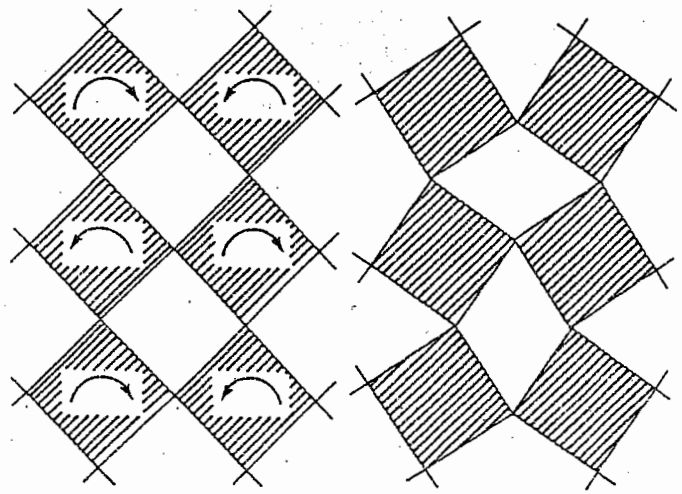

Figure 15 Schematic drawing of an elastic phase transition of the $SrTiO_3$-type in a perovskite structure. The local state variable is the rotation angle, the K-tensor is due to the hinges of the oxygen atoms.

the analogue of the forces shown in Fig. 1b and symbolized by $K$ in Eq. 1. The forces will be transmitted to neighbouring octahedra as discussed in sections 1 and 2, resulting in the tetragonal structure of Fig. 10b which can be considered as an ordering of the $\theta_i$ variables. Another example with a similar 'rigid unit mode' is the $\propto/\beta$ phase transition in quartz in which the corner sharing $SiO_4$ tetrahedra rotate (Dove, Giddy and Heine, 1993; Salje, Ridgwell, Guttler, Wruck, Dove and Dolino, 1992). In this case one can make domain walls perpendicular to the $a^*$ axis which involves only rotations and displacements of the tetrahedra without distortion. These walls are therefore analogous to the Type 1 walls and form the triangular domain pattern or incommensurate phase over a small temperature interval at the $\propto/\beta$ phase boundary. This example shows both the similarities to our model and the difference of detail in so far as we have boundaries analogous to those of Type 1 in Section 5 but occurring in quartz, which is antiferroelastic. The latter difference from our simple cubic model arises from the difference in structure.

*Acknowledgements*

The computer simulations were carried out on the Cambridge University Distributed Array Processor partially funded by the (British) Science and Engineering Research Council. Work supported by NERC.



*References*

Aizu, K. (1970). Deformination of state parameters and formulation of spontaneous strain for ferroelastics. *J. Phys. Soc. Jap.*, **328**, 706.

Barsch, G.R. and J.A. Krumhansl (1984). Twin boundaries in ferroelastic media without interface dislocations. *Phys. Rev. Lett.*, **53**, 1069.

Barsch, G.R. and J.A. Krumhansl (1988). Nonlinear and nonlocal continuum model of transformation precursors in martensites. *Met. Trans.*, **19A**, 761.

Bilby, B.A. and J.W. Christian (1956). *The Mechanism of Phase Transformations in Metals, Inst. of Metals, London.*

Bismayer, U. and E. Salje (1981). Ferroelastic phases in $Pb_3(P0_4)_2$-$Pb_3(AsO_4)_2$ X-ray and optical experiments. *Acta. Cryst.* **A37**, 145.

Bismayer, U., E. Salje and C. Joffrin (1982). Reinvestigation of the stepwise character of the ferroelastic phase transition in lead phosphate-arsenate, $Pb_3(PO_4)_2$-$Pb_3(AsO_4)_2$ *J. Physique*, **43**, 1379.

Bratkovsky, A., E. Salje, S . Marais and V. Heine (1993). Theory of fluctuations and texture embryos in structural phase transitions mediated by strain. *J. Phys. Condens. Matter* (in preparation).

Bratkovsky, A.M., E. Salje, S.C. Marais and V. Heine (1993). Theory and computer simulation of tweed texture, Phase Trans. (in press).

Bratkovsky, A.M., E. Salje and V. Heine (1993). Theory and simulation of the origin, form and coarsening of tweed texture. Europhys. Lett., in preparation.

Christian, J.W. (1965). *The Theory of Phase Transformations in Metals and Alloys, Pergamon Press, Oxford.*

Christian, J.W. (1990). Analysis of lattice and shape deformations and of atomic shuffles in martensitic-transformation. *Mat. Sci. Eng.*, **A127**, 215.

Clapp, P.C. (1990). The critical role of defects in 1st-order displacive transformations. *Mat. Sci. Eng.*, **A127**, 189.

Cook, H.E. and D. de Fontaine (1969). On the elastic free energy of Solid solutions I. microscopic theory. *Acta. Met.* **17**, 915.

Cowley, R.A. (1976). Acoustic phonon instabilities and structural phase transitions. *Phys. Rev.* **B13**, 4877.

Cross, L.E. (1987). Relaxor ferroelectrics. *Ferroelectrics*, **76**, 241.

Dattagupta, S., V. Heine, S. Marais and E. Salje (1991). Rate equation for atomic ordering in mean field theory I: uniform case. *J. Phys. Cond. Matter*, **3**, 2963.

Dove, M.T. and B.M. Powell (1989). Neutron-diffraction study of the tricritical orientational order-disorder phase-transition in calcite at 1260-K. *Phys. Chem. Min.* **16**, 503.

Dove, M.T., A.P. Giddy and V. Heine (1993). Rigid unit modes of displacive phase transitions in framework silicates. *Trans. Amer. Crystal. Assoc.*, **27**, in press.

Finlayson, T.R. (1988). Pretransformation phenomena as revealed by elastic-waves. *Phys. Metall. Mater. Sci.*, **19A**, 185.

Fleury, P.A., J.F. Scott and J.M. Worlock (1968). Critical dynamics of elastic phase transitions. *Phys. Rev. Lett.*, **21**, 16.

Folk, F., H. Iro, and I. Schwabl (1979). Critical dynamics of elastic phase transitions. *Phys. Rev.*, **B20**, 1229.

Ginzburg, V.L. and L.D. Landau (1950). On the theory of superconductivity. *Zh. Eksp. Theor. Fiz.*, **20**, 1064.

Gooding, R.J. (1990). Anharmonicity and martensitic instabilities in beta-cubic structures. *Mat. Sc. Eng.*, **A127**, 183.

Gridnev, S .A., L.A. Shuvalov and V.V. Bondarenko (1985). Study of ferroelectric phases that intermediate between alpha and beta ones in $NaH_3(SeO_3)_2$ crystal. *Sov. Phys. Sol. State*, **27**, 283.

Gunton, J.D., E.T. Gawlinski, A. Chakrabarti and H. Kaski (1988). Numerical simulation of models of ordering — scaling and growth laws. *J. Appl. Crystallogr.*, **21**, 811.

Harris, M.J., E. Salje, B.K. Guttler and M.A. Carpenter (1989). Determination of the degree of Al.Si order $Q_{od}$ in kinetically disordered albite using hard mode infrared spectroscopy. *Phys. Chem. Min.*, **16**, 649.

Khatchaturyan, A.G. (1966). Some questions of the theory of phase transformation in solids. *Fiz. Tverd. Tela (Leningrad)*, **8**, 2709.

Khatchaturyan, A.G. (1983). *Theory of Structural Transformations in Solids*, Wiley, New York.

Knorr, K., A. Loidl and J.K. Kyems (1986). Ferroelastic transition in KBr-KCN studied by neutrons. X-rays and ultrasonics. *Physica*, **B136**, 311.

Krekels, T., G. Van Tendeloo, D. Broddin, S. Amelinckx, L. Tanner, M. Mekbod, E. Vaniathem and R. Deltour (1991). Tweed Structure of Fe-doped $YBa_2Cu_3O_{7-\delta}$. *Physica*, **C173**, 361.

Kriven,W.M. (1990). Martensitic toughening of ceramics *Mat. Sci. Eng.*, **A127**, 249.

Kroll, H. and P. H. Ribbe (1987). Determining (Al, Si) distribution and strain in alkali feldspars using lattice-parameters and diffraction-peak positions — a review. *Am. Min.*, **72**, 491.

Krumhansl, J.A. and Y. Yamada (1990). Some new aspects of 1st-order displacive phase-transformations — martensites. *Mat. Sc. Eng.*, **A127**, 167.

Lynden-Bell, R.M., M. Ferrario, I.R. McDonald and E. Salje (1990) A molecular dynamics study of orientational disordering in crystalline sodium nitrate. *J. Phys. Condens. Matter*, 1, 6523.

Maeda, M. (1988). Elastic, dielelectric and optical-properties of ferroelectric betaine arsenate. *J. Phys. Soc. Jap.*, **57**, 2162.

Marais, S., V. Heine, C. Nex and E. Salje (1991). Phenomena due to strain coupling in phase transitions. *Phys. Rev. Lett.*, **66**, 2480.

Marais, S. and E. Salje (1991). Derivation of a rate law for non-uniform systems and continuous order parameters. *J. Phys. Cond. Matter*, **3**, 3667.

Marais, S., A. Bratkovsky, V. Heine and E. Salje (1993). Strain coupling as the dominant interaction in structural phase transitions. *Phys. Rev.* **B** (in preparation).

Mayer, A.P. and R.A. Cowley (1988). The influence of random stresses on the scattering of a crystal with a planar elastic instability. *J. Phys.*, **C21**, 483.

Mayer-Botzel, H. and H. Wagner (1988). Hydrogen density modes and coherent phase transition in $NbH_x$. *Z. Physik*, **B72**, 101.

McLaren, A.C. and J.D. Fitzgerald (1987). Cbed and Alchemi investigation of local symmetry and Al,Si ordering K-feldspars. *Phys. Chem. Min.*, **14**, 281.

Negita, K. (1989). Lattice-vibrations and cubic to tetragonal phase- transition in $ZrO_2$. *Acta. Metall.*, 37, 313.

Nord, G.L. and C.A. Lawson (1989). Order-disorder transition induced twin domains and magnetic-properties in ilmenite-hematite. *Am. Min.*, 74, 160.

Orgzall, I. and B . Lorenz (1990). Computer-simulation of cluster-size distributions in nucleation and growth-processes. *Acta. Metall.*, **36**, 627.

Palmer, D.C. and E. Salje (1990). Phase transitions in leucite: Dielectrie properties and transition mechanism. *Phys. Chem. Min.*, **17**, 9.

Palmer, D.C., A. Putnis and E. Salje (1988). Twinning in tetragonal leucite. *Phys. Chem. Min.* **16**, 298.

Parlinski, K., E. Salje and V. Heine (1993). Annealing of tweed microstructure in high-$T_c$ superconductors studied by computer simulation, *Acta Metall. Mater.*, *41*, 839.

Parlinski, K., V. Heine, E. Salje (1993). Origin of tweed texture in the simulation of a cuprate superconductor, *J. Phys. Condens. Matter*, **5**, 497.

Plakida, N.M. and W. Saleyeva (1988). The improper ferroelastic phase- transition in superionic $Rb_3h(SeO_4)_2$ crystals. *Phys. Stat. Sol.*, **B148**, 473.

Powell, B.M. and P.N. Gerlach (1989). Soft-mode transition in the ferroelastic crystal $K_2Hg(Cn)_4$. *Phys. Rev.*, **B40**, 2426.

Putnis, A., E. Salje, S.A.T. Redfern, C.A. Fyfe and H. Stroble (1987). Structural states of Mg cordierite I: order parameter from synchrotron X-ray and NMR data. *Phys. Chem. Min.*, 14, 446.

Redfern, S.A.T., A. Graeme-Barber and E. Salje, (1988). Thermodynamics of plagioclase III: spontaneous strain at the $I\bar{1}-P\bar{1}$ phase transition in Ca-rich plagioclase. *Phys. Chem. Min.*, **16**, 157.

Ribbe, P.H. (1983). Feldspar mineralogy. *Rev. Min. Soc. Am.*, **2**, 1.

Salje, E. (1987). Structural states of Mg cordierite II: Landau theory. *Phys. Chem. Min.*, 14, 455.

Salje, E. (1988). Kinetic rate laws as derived from order parameter theory I: theoretical concepts. *Phys. Chem. Min.*, **15**, 336.

Salje, E. (1990). Phase transitions in ferroelastic and co-elastic crystals. *Ferroelectrics*, **104**, 111.

Salje, E. (1991). Crystallography and structural phase transitions, an introduction. *Acta. Cryst.*, **A47**, 453.

Salje, E. (1992a). Phase transitions in minerals: from equilibrium properties towards kinetic behaviour. *Berichte der Bunsengesellschaft fur physikalische Chemie*, **96**, 1518.

Salje, E. (1992b). Application of Landau theory for the analysis of phase transitions in minerals. *Physics Reports*, **215**, 49.

Salje, E. (1993). *Phase Transitions in Ferroelastic and Co-Elastic Crystals, Cambridge University Press, Cambridge, UK.*

Salje, E. and B. Wruck (1983). Specific heat measurements and critical exponents of the ferroelastic phase transition in $Pb_3(PO_4)_2$ and $Pb_3(P_xAs_{1-x}O_4)_2$. *Phys. Rev.*, **28**, 6510.

Salje, E., A. Graeme-Barber, M.A. Carpenter and U. Bismayer. (1993). Lattice parameters, spontaneous strain and phase transitions in $Pb_3(PO_4)_2$. *Acta Cryst.*, in print.

Salje, E., A. Ridgwell, B. Guttler, B. Wruck, M.T. Dove and G. Dolino, (1992). On the displacive character of the phase transition in quartz: A hard mode spectroscopy study. *J. Phys. Conden. Matter.*, **4**, 571.



Salje, E., B. Palosz and B. Wruck (1987). In-situ observation of the polytypic phase transition 2H-12R in $PbI_2$: investigation of the thermodynamic structural and dielectric properties. *J. Phys. Condens. Matter*, **20**, 4077.

Salje, E. and K. Parlinski, (1991). Microstructures in the high-$T_c$ Superconductors. *Supercond. Sc. Techn.*, **4**, 93.

Salje, E. and S. Marais (1992). On the correlation between local potentials and the thermodynamic/kinetic behaviour of ferroelectrics, *Ferroelectrics*, **136**, 1.

Salje, E. and U. Bismayer (1989). Order parameter behaviour in the relax or ferroelastic lead scandium tantalate. *J. Phys. Condens. Matter*, **1**, 6967.

Salje, E., V. Devarajan, U. Bismayer and D.M.C. Guimaraes (1983). Phase transitions in $Pb_3(P_{1-x}As_xO_4)_2$: influence of the central peak and flip mode on the Raman scattering of hard modes. *J. Phys*, C16, 5233.

Sapriel, J. (1975). Domain wall orientation in ferroelastics. *Phys. Rev.*, **B12**, 5128.

Schmahl, W.W., A. Putnis, E. Salje, P. Freemann, A. Graeme-Barker, R. Jones, K.K. Singh, J. Blunt, P.P. Edwards, J. Loram and K. Mirza (1989). Twin formation and structural modulations in orthorhombic and tetragonal $YBa_2(Cu_{1-x}Co_x)_3O_{7-\delta}$. *Phil. Mag. Lett.*, **60**, 241.

Silverstein, A. and P.C. Clapp (1988). Modeling and interpretation of tweed microstructures in face-centered-cubic solids. *Phys. Rev.*, **B38**, 9555.

Tanner, L.E. and M. Wuttig (1990). Workshop on 1st-order displacive phase-transformations — review and recommendations. *Mat. Sci. Eng.*, **A127**, 137.

Tautz, F.S., V. Heine, M.T. Dove and X. Chen (1991). Rigid unit modes in the molecular dynamics simulation of quartz and the incommensurate phase transition. *Phys. Chem. Min.*, **18**, 326.

Van Tendeloo, G., S. Ghose and S. Amelinckx (1989). A dynamical model for the $P\bar{1}-I\bar{1}$ phase-transition in anorthite, $CaAl_2Si_2O_8$1. Evidence from electron-microscopy. *Phys. Chem. Min.*, **16**, 311.

Wadhawan, K.K. (1982). Ferroelasticity and related properties of crystals. *Phase Trans.*, **3**, 3.

Wagner, H. (1988). *Hydrogen in Metals. Springer, Heidelberg.*

Weber, H.P., B.C. Topfield and P.F. Liabo (1975). Ferroelastic behaviour and the monoclinic-to-orthorhombic phase transition in $MP_5O_{14}$ (M = La – Tb). *Phys. Rev.*, **B11**, 1152.

Wen, S.H., A.G. Khatchaturyan and J.W. Morris (198l). Computer simulation of a "tweed-transformation" in an idealized elastic crystal. *Met. Trans.*, **A12**, 581.

Wruck, B., E. Salje and A. Graeme-Barber (1991). Kinetic rate laws derived from order parameter theory IV: Kinetics of Al-Si disordering in Na- feldspars. *Phys. Chem. Min.*, **17**, 700.